Catalysis Letters 19 (1993) 67–79

Synthesis and catalytic properties of substituted $AlPO_4$-31 molecular sieves

H.-L. Zubowa, M. Richter [1], U. Roost, B. Parlitz and R. Fricke

Zentrum für Heterogene Katalyse, Rudower Chaussee 5, D-1199 Berlin-Adlershof, Germany

Received 14 October 1992; accepted 3 March 1993

Molecular sieve $AlPO_4$-31 and substituted analogues (MnAPO-31, SAPO-31, MnAPSO-31) have been tested for their catalytic properties in the isomerization of 1-butene over 6 h time on stream at 743 K. The conversion of 1-butene proceeds selectively by either double bond or skeletal isomerization. MnAPSO-31 with a molar MnO/P_2O_5 ratio adjusted to 0.01 yields the highest percentage of isobutene whereas the parent $AlPO_4$-31 leads almost completely to a double bond shift with only minor skeletal isomerization. The results are related to the acidity characteristics that were determined by ammonia thermodesorption. Deactivation is accompanied by a loss of selectivity for the skeletal isomerization.

Keywords: Aluminophosphate molecular sieves; Si and/or Mn modification; isomerization of 1-butene

1. Introduction

Aluminophosphate molecular sieves ($AlPO_4$) are a new class of microporous solids with great varieties of crystal structures and chemical compositions [1–7]. They possess not only the characteristic features of zeolites but also additional specific properties owing to their chemical constituents. Aluminophosphate molecular sieves are built from aluminate and phosphate tetrahedra: their lattice is electroneutral with neither nonframework cations nor ion exchange capacity. An isomorphous replacement of P and/or Al by other elements opens wide possibilities for modifying the $AlPO_4$s in terms of their acidity (creation of acid sites of Brønsted type with different acid strengths) and also, although relatively minor, in terms of alterations of pore radii. Silicoaluminophosphates (SAPOs) are formed after a partial substitution of lattice phosphorus by silicon; manganese aluminophosphates (MnAPOs) are formed after partial replacement of lattice aluminum by manganese. A simultaneous presence of both silicon and manganese in the synthesis gel leads to manganese silicoaluminophosphates (MnAPSOs).

[1] To whom correspondence should be addressed.

The well defined system of pores with diameters between 0.3 and 1.0 nm favors applications of these molecular sieves as catalyst components and adsorbents. Their shape selective catalytic properties emerge due to the variety of pore sizes and shapes. $AlPO_4$-31 belongs to the class of medium pore molecular sieves and has an unidimensional pore system ($d = 0.53$ nm) whose 12-ring pore openings are circular, built from alternating 4- and 6-rings. According to Bennett and Kirchner [7] the difference in pore size compared to $AlPO_4$-5 ($d = 0.73$ nm), another molecular sieve with circular 12-ring pores, results from the zigzag chains that tilt the 4-rings and produce extremely nonplanar 6-rings in $AlPO_4$-31. The unit cell parameters are $a = b = 2.083$ nm, $c = 0.50$ nm, and $\gamma = 120°$ [7].

Synthesis and properties of the molecular sieve SAPO-31 were described in a previous paper [8]. It could be shown by ^{27}Al and ^{31}P MAS NMR that aluminum and phosphorus are tetrahedrally coordinated in the dehydrated framework. According to ^{29}Si MAS NMR only a part of the silicon is incorporated into the framework in the form of monomeric silicon, the remainder being present as amorphous material and/or silica islands within the SAPO-31 framework. This contribution reports on the synthesis of $AlPO_4$-31 and its substituted analogues, MnAPO-31 and MnAPSO-31, as well as on their catalytic properties for the isomerization of 1-butene.

The conversion of 1-butene into isobutene is of great technical interest, because isobutene is one component for manufacturing methyl tertiary-butyl ether (MTBE) which is a valuable octane rate booster for gasoline. In general, butenes are obtained from cracking units as mixtures containing 1-butene, cis-, trans-2-butene, isobutene, *n*- and isobutane as well as butadiene. Butadiene and isobutene are valuable raw materials, separated from the C_4 cut by extraction (butadiene) or through a MTBE synthesis stage (isobutene). The feed can be recycled for further isomerization of *n*-butenes to isobutene. Normally, the conversion is performed as heterogeneously catalyzed gas phase reaction within the temperature range 600–900 K over acid solids, preferentially silica–alumina [9] or η- and γ-Al_2O_3 promoted with HF [10]. A serious drawback of the latter catalyst system is the volatile fluor compound and the short lifetime of the catalyst.

The skeletal isomerization of 1-butene at elevated temperatures is always accompanied by a double bond isomerization to cis- and trans-2-butene which are mutually interconvertible. The reaction scheme can be visualized as shown in fig. 1a. Fig. 1b represents the thermodynamic equilibrium composition of a C_4 olefin mixture between 300 and 1000 K [11]. From a thermodynamic standpoint the percentage of isobutene is highest at low temperatures but to achieve reasonable reaction rates in the technical process, higher temperatures are required.

We examined the conversion of 1-butene into isobutene over $AlPO_4$-31 modified with either Si (SAPO-31) or Mn (MnAPO-31) or both elements (MnAPSO-31) during the synthesis stage. The results are related to the acidity characteristics of the molecular sieves.

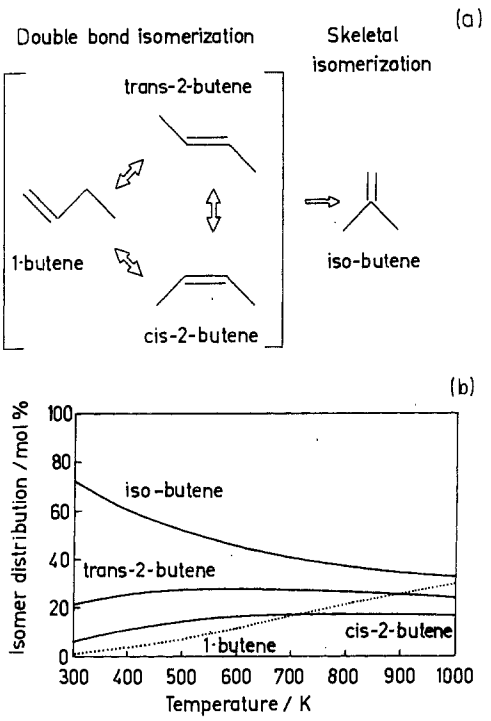

Fig. 1. Isomerization of *n*-butenes. (a) Reaction scheme, and (b) thermodynamic equilibrium composition between 300 and 1000 K [11].

2. Experimental

2.1. SYNTHESIS OF THE MOLECULAR SIEVES

The parent molecular sieve $AlPO_4$-31 was synthesized according to the method described by Lok et al. [12] but with those alterations outlined in ref. [8]. The gel had the composition (on a molar basis): 3.0 Pr_2NH (di-*n*-propylamine), 1.2 Al_2O_3, 1.0 P_2O_5, 40 H_2O. The crystallization was performed under autogenous pressure at 473 K within a teflon-lined steel autoclave (volume 100 cm^3) for a synthesis time of 24 h.

After crystallization had been completed the solid was separated from the mixture, washed with distilled water until neutrality and dried at room temperature under ambient conditions. Finally, the molecular sieve was calcined at 873 K in air. The XRD pattern confirms the phase purity (fig. 2a, dashed spectrum). However, a synthesis procedure employing template excess leads to large crystal agglomerates up to diameters of 200 μm (fig. 3a). For catalytic applications, small crystallites guarantee better effectiveness owing to a favourable surface-to-volume ratio. The morphology has been found to be dependent on the template concentration in the gel. Synthesis performed with only 1 mol Pr_2NH instead of 3 mol supported by a small amount of $AlPO_4$-31 seed crystals yield $AlPO_4$-31 molecular sieve crys-

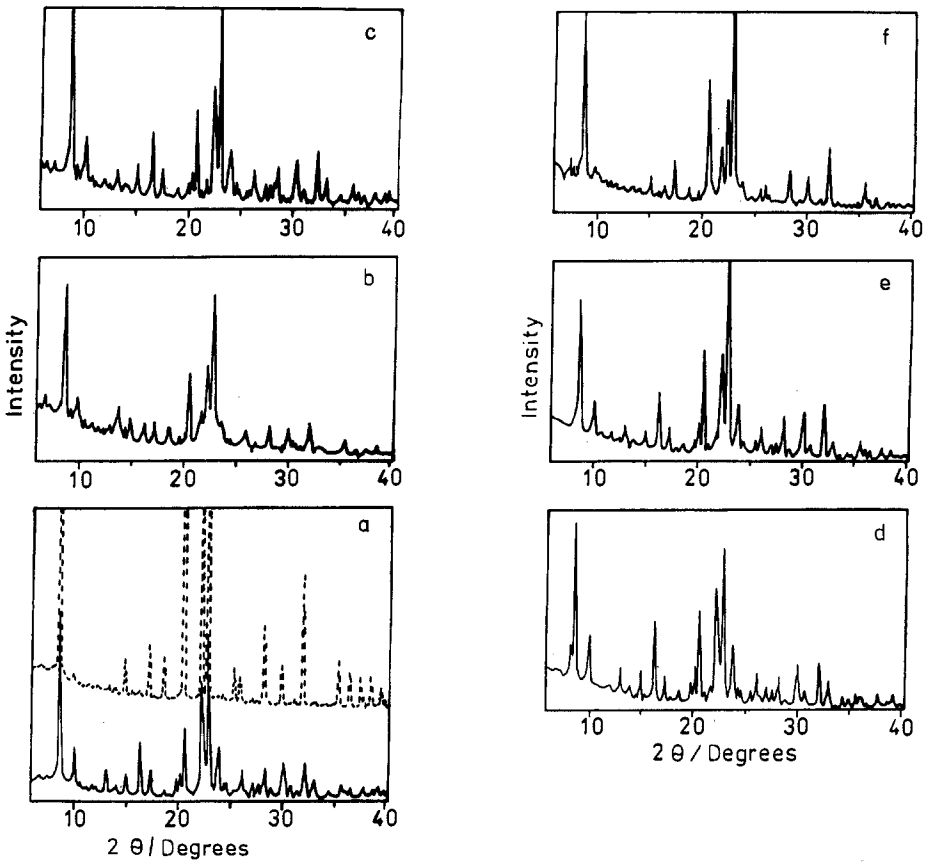

Fig. 2. XRD Patterns of $AlPO_4$-31 based molecular sieves. (a) $AlPO_4$-31, synthesized with template excess (– – –) and with low template concentration (——), (b) MnAPO-31/2, (c) SAPO-31, (d) MnAPSO-31/1, (e) MnAPSO-31/2, and (f) MnAPSO-31/3.

tals of smaller size (fig. 3b) but simultaneously some admixture of a second phase identified as $AlPO_4$-11 is observed (fig. 2a, full lines). Since the investigation had an industrial background [13] The phase impurity, which is present in the substituted analogues as well, was tolerated. Synthesis on a larger scale, above all, has to avoid large amounts of the amine templates for economic and environmental reasons.

SAPO-31, MnAPO-31 and MnAPSO-31 were synthesized from a gel of the molar composition 1.0 Pr_2NH, 1.2 Al_2O_3, 1.0 P_2O_5 and 40 H_2O. Additionally, SiO_2-sol and/or $MnSO_4$ H_2O were added. All syntheses were supported by addition of $AlPO_4$-31 seed crystals.

The analytical determination of the manganese content was performed photometrically at a wavelength of 450 nm [14]. The manganese was brought into solution by boiling 50–100 mg of the samples with concentrated HCl for 10 min. Afterwards, solutions for photometrical analysis were prepared according to analytical standards [14]. Table 1 summarizes designations, compositions and overall acidities of the molecular sieve samples.

Table 1
Catalyst samples

Notation	MnO/P_2O_5 ratio	SiO_2/P_2O_5 ratio	Mn content (wt%)	Overall acidity (mmol/g)
$AlPO_4$-31	–	–	–	0.15
MnAPO-31/1[a]	0.025	–	0.75	0.26
MnAPO-31/2	0.010	–	0.32	0.23
SAPO-31	–	0.1	–	0.26
MnAPSO-31/1	0.010	0.1	0.28	0.25
MnAPSO-31/2	0.025	0.1	0.65	0.25
MnAPSO-31/3	0.050	0.1	1.25	0.24

[a] Reference sample that was used in ammonia TPD for allowing comparison of acidity with sample MnAPSO-31/2.

2.2. CHARACTERIZATION OF THE MOLECULAR SIEVES

The molecular sieves were characterized by X-ray diffraction (Cu K_α-radiation) within the range $2.2° < \theta < 20°$. Scanning electron microscopy was performed with a Tesla BS 300 equipment.

Temperature programmed desorption of ammonia (NH_3 TPD) was carried out at normal pressure in a flow reactor with helium (carrier gas flow rate 1 $cm^3\ s^{-1}$). After the adsorption step of ammonia at 393 K, the heating program consisted of an isothermal desorption at 393 K followed by a linear temperature increase (heating rate 10 K min^{-1}) up to 800 K. The desorption was completed under isothermal conditions at 800 K. Sample weights of 200 mg were used (crushed pellets, 0.35–1.0 mm). Desorbing H_2O was removed by a KOH trap before analysis. The gas phase concentration of NH_3 was determined by a thermal conductivity cell. Additionally, the effluent stream was conducted through a water flask and the overall amount of desorbed ammonia analysed after completion of the experiment by titration with 0.1 N H_2SO_4. The overall concentration of acid sites corresponds to the amount of desorbed ammonia. A discrimination between strong (Brønsted) sites and weak (Lewis) sites through deconvolution of the desorption profiles could not be performed owing to the poor resolution.

2.3. CATALYSIS

Catalytic measurements were performed under normal pressure at 743 K applying a feed containing 50% of 1-butene, diluted by nitrogen (overall flow rate 1 $cm^3\ s^{-1}$) in a metal flow reactor (diameter 10 mm). Catalyst extrudates (diameter $\sim$ 1.5 mm) were prepared from the template-free molecular sieve (35%) and a binder (65%, SiO_2/Degussa). Catalyst weights of 1 g were used for the catalytic tests. Therefore, the weight hourly space velocity (WHSV) amounted to 4.5 h^{-1} (gram of 1-butene per gram of catalyst per hour) at the chosen reaction conditions. The first

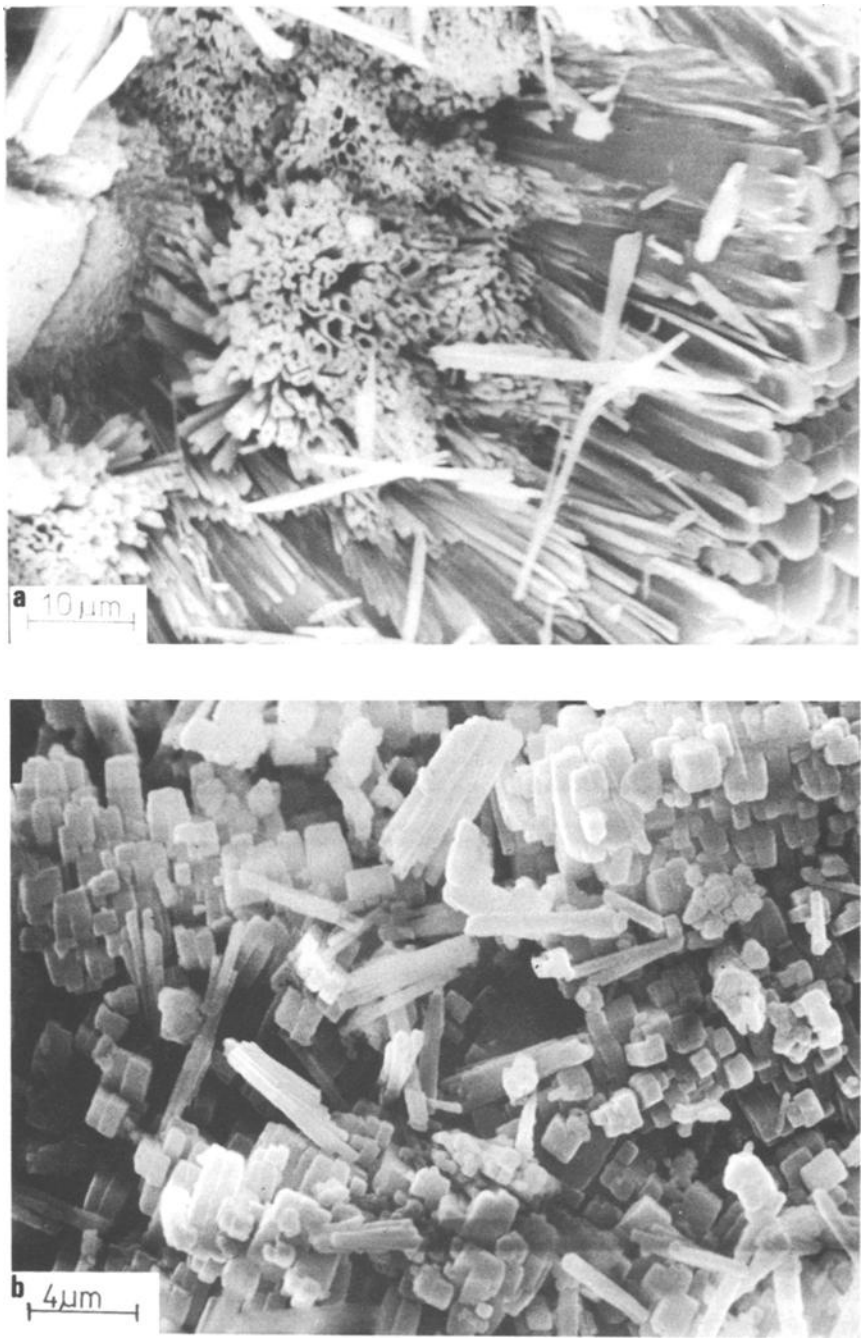

Fig. 3. Scanning electron micrographs of (a) $AlPO_4$-31, synthesized with high template concentration, (b) $AlPO_4$-31, low template concentration, (c) SAPO-31, and (d) MnAPSO-31/2.

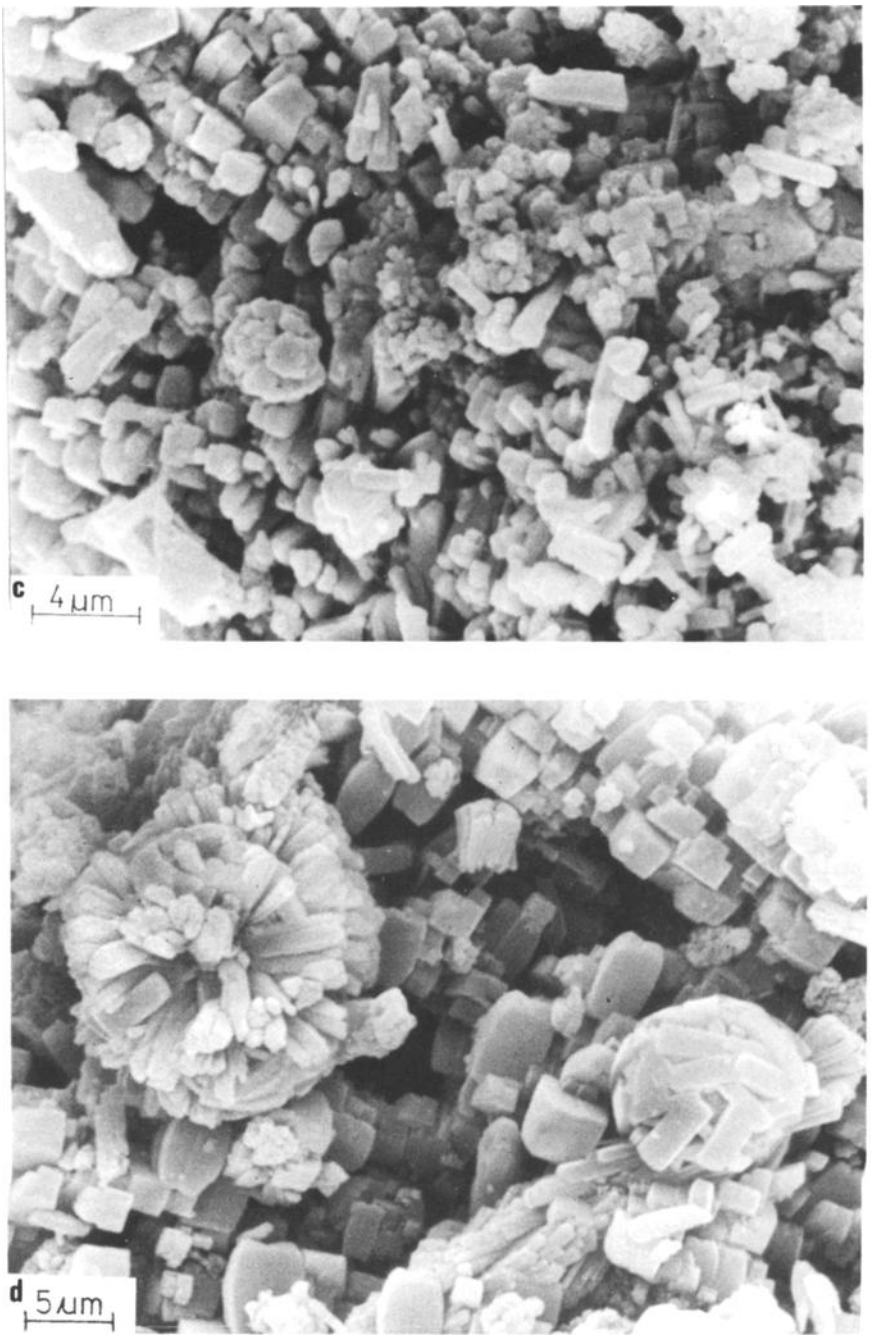

Fig. 3. Continued.

analysis was performed after 0.5 h time on stream, the second one after 1 h and further analyses were taken in regular intervals up to 6 h. Catalytic data were evaluated as follows:

$$\text{conversion of 1-butene (\%)} = 100[(\text{1-butene})_{in} - (\text{1-butene})_{out}]/(\text{1-butene})_{in},$$
$$\text{selectivity of isobutene (\%)} = 100(\text{isobutene})_{out}/[(\text{1-butene})_{in} - (\text{1-butene})_{out}],$$

referred to the overall conversion of 1-butene.

Product analysis was accomplished by gas chromatography on packed beds of Kugelgel KW 1 (column length 2 m, internal diameter 2.4 mm) at 353 K (separation of 1-butene from isobutene and *n*-butenes) and porolith with 15% di-*n*-propylsulfone (column length 4 m, internal diameter 2.4 mm) at 298 K (separation of products).

3. Results and discussion

3.1. CRYSTALLINITY AND MORPHOLOGY

Both the as-synthesized and the template-free synthesis products were characterized by XRD. All samples exhibit the $AlPO_4$-31 structure. The XRD diagram of the parent $AlPO_4$-31 synthesized with template excess is given in fig. 2a (dashed). Characteristic X-ray diffraction lines are observed at d = 0.282, 0.320, 0.393, 0.406, 0.440 and 1.030 nm. Fig. 2a (full lines) shows the XRD pattern received for $AlPO_4$-31 synthesized with low template concentration. The emergence of additional lines is easily seen by comparison with the dashed spectrum. The alien phase could be identified as $AlPO_4$-11. Its content reaches ~15%. The Si and Mn substituted analogues all contain some admixture of the 11 structure, yet the percentage varies as estimated from the intensity ratio of the characteristic diffraction lines (figs. 2b–2f).

As mentioned before, $AlPO_4$-31 crystallites from as-synthesized batches with high template concentration have spherical shape with maximum diameters of ~ 200 μm. These spherical particles are agglomerates with at least three layers of varying morphology (fig. 3a): the outer layer consists of hexagonal compact bars and needles, the intermediate layer is built from hexagonal pipes, and the core has apparently a more dense consistency. The $AlPO_4$-31 sample utilized for catalytic measurements reveals a different morphology (fig. 3b). The rod-shaped, predominantly agglomerated crystallites exhibit average dimensions of 3 × 1 × 1 μm. In principle, SAPO-31 and MnAPSO-31 have similar morphologies (figs. 3c, 3d). Agglomerates reach diameters up to 15 × 15 μm (MnAPSO-31/2).

3.2. ACIDITY

The ammonia desorption profile of $AlPO_4$-31 shows a single asymmetric peak

with a maximum temperature at 498 K (fig. 4a and table 1). The acidity originates from either Lewis acid sites or terminal POH groups which could be shown to exist on $AlPO_4$-31 [15]. POH groups represent weak acid sites of Brønsted type. Sites with higher acid strength are generated if, at least partially, Al(III) is replaced by Mn(II) (MnAPO structure) or P(V) is replaced by Si(IV) (SAPO structure). Obviously, both substitution routes have taken place as infers from the ammonia desorption profiles of MnAPO-31/2 and SAPO-31 (figs. 4a, 4b). The MnAPO-31 structure reveals an enhanced overall acidity compared with $AlPO_4$-31 including a certain percentage of sites with higher acid strength that characterizes the peak form beyond 550 K. Direct evidence for manganese incorporation into molecular sieve structure $AlPO_4$-11 is reported by Brouet et al. [16] who applied electron spin-echo modulation measurements. In our case, indirect evidence for a partial incorporation of Mn(II) in framework positions of $AlPO_4$-31 comes from ammonia

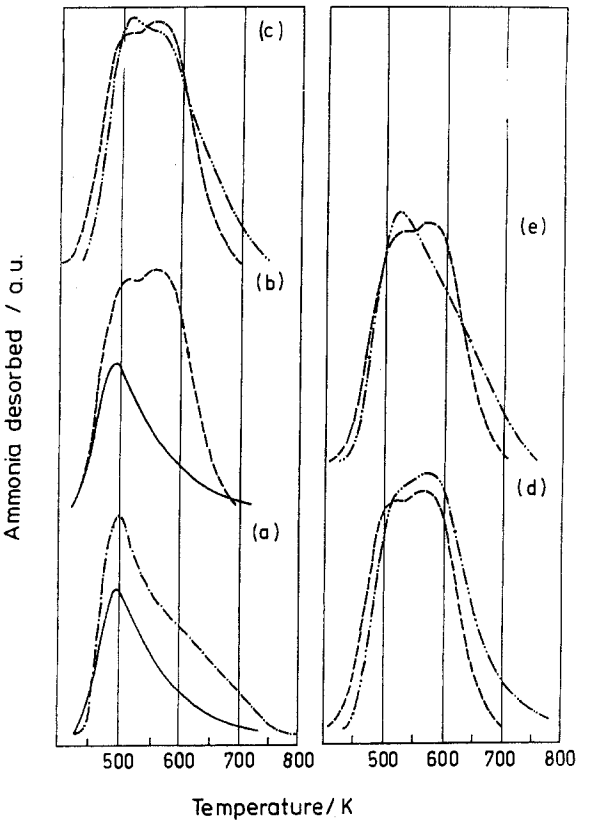

Fig. 4. Ammonia TPD profiles following adsorption at 393 K. (a) $AlPO_4$-31, low template concentration (——) and MnAPO-31/1 (– · –), (b) $AlPO_4$-31 (——) and SAPO-31 (– – –), (c) SAPO-31 (– – –) and MnAPSO-31/2 (– · · –), (d) SAPO-31 (– – –) and MnAPSO-31/1 (– · · –) and (e) SAPO-31 (– – –) and MnAPSO-31/3 (– · · –). Sample weight 0.2 g, carrier gas helium, flow rate 1 $cm^3\ s^{-1}$, heating rate 10 K min^{-1}.

desorption and from the observed activity enhancement of the MnAPO-31/2 sample during the skeletal isomerization of 1-butene (see later). The modification of the parent $AlPO_4$-31 by Si(IV) leads to a profile indicating a pronounced increase of acidity, where two desorption peaks can be distinguished, although poorly resolved (fig. 4b).

The acidic properties of the MnAPSO-31 samples are clearly dominated by the Si(IV) in lattice positions. Therefore, the ammonia desorption profile of sample MnAPSO-31/2 (fig. 4c) whose Mn content is nearly identical to that of sample MnAPO-31 shows only minor modifications compared with SAPO-31. However, the form of the ammonia desorption profile and hence the acid site population seems to depend systematically on the Mn concentration (figs. 4c–4e). A higher Mn content (sample MnAPSO-31/3) leads to a partial deterioration of Brønsted acidity (fig. 4e). Naturally, the incorporation of manganese cations (and also of silicon) in lattice positions is limited. Any excess leads unevitably to a deposition of manganese species outside the lattice. It can be assumed that beyond a certain threshold concentration these manganese species are transformed into an oxidic phase through the calcination procedure. Additionally, this may affect the shape of the ammonia desorption profiles. The loss of Brønsted acid sites can occur by different processes:

(i) Manganese disturbs the crystal growth during the synthesis stage and thus renders the formation of Brønsted sites more difficult.

(ii) Nonframework manganese species neutralizes partly the acidity by some kind of salt formation.

(iii) Manganese cations (in the form of $MnOH^+$ or similar species) replace protons of Brønsted acid sites by ion exchange.

In view of the catalytic effects an optimum manganese concentration should exist where the reaction benefits from the tuned acidity but does not suffer from the blockage of acid sites by excess manganese.

3.3. THE REACTION

The catalytic performance of the various molecular sieves after 6 h time on stream are compared in table 2. Material balances were always better than 90%. A comparison of the experimentally observed distribution of butenes with thermodynamic values at 743 K (18.2% 1-butene, 17.0% cis-2-butene, 26.4% trans-2-butene and 38.4% isobutene, fig. 1b) shows that all catalyst samples, with exception of the parent $AlPO_4$-31 structure, operate near thermodynamic equilibrium as far as the 1-butene conversion is concerned. For achieving high yields of isobutene, the isomerization route has to be shifted from double bond to skeletal isomerization. In principle, the parent $AlPO_4$-31 structure should not be able of catalyzing any hydrocarbon reaction owing to its electroneutral composition that excludes the existence of Brønsted acid sites. However, we have shown in ref. [15] that the acid

Table 2
Isomerization of 1-butene over substituted $AlPO_4$-31 molecular sieves [a]

Molecular sieve	Conversion of 1-butene (%)	Selectivity of isobutene (%)	Product composition (vol%) [b]			
			1-	cis-2-	trans-2-	iso
$AlPO_4$-31	69.8	6.6	30.2	28.0	35.2	4.6
MnAPO-31/2	73.4	19.1	26.6	24.6	31.2	14.0
SAPO-31	73.6	26.3	26.4	22.8	28.8	19.4
MnAPSO-31/1	76.6	32.9	23.4	21.6	27.8	25.2
MnAPSO-31/2	75.4	25.7	24.6	23.6	30.2	19.4
MnAPSO-31/3	71.9	14.2	28.2	26.2	33.2	10.2

[a] Catalytic data at $T = 743$ K after 6 h time on stream. Catalyst weight 1.0 g (35 wt% molecular sieve, 65 wt% SiO_2 binder), feed composition 50 vol% 1-butene, 50 vol% nitrogen, overall flow rate 1 $cm^3 s^{-1}$, WHSV = 4.5 h^{-1}.

[b] Only the butenes are condidered. Analysis of liquid products accumulated over 6 h in the case of SAPO-31 shows that linear and branched higher alkenes and, to a minor extent, substituted benzenes are formed besides isomerization.

strength of the existing terminal POH groups is high enough to allow double bond and, to a minor extent, skeletal isomerization of *n*-butenes.

A modification of the parent $AlPO_4$-31 structure by either Mn or Si improves the isobutene selectivity. This is attributed to the creation of Brønsted acid sites via replacement of lattice atoms. The better catalytic performance of SAPO-31 corresponds to the higher concentration of acid sites and presumably to the higher acid strength of these sites. Acid sites releasing preadsorbed ammonia at temperatures beyond 550 K seem to be of primary importance for the skeletal isomerization. The simultaneous presence of Mn and Si leads to a further improvement provided the content of the former is kept around 0.3 wt% (sample MnAPSO-31/1). It cannot be

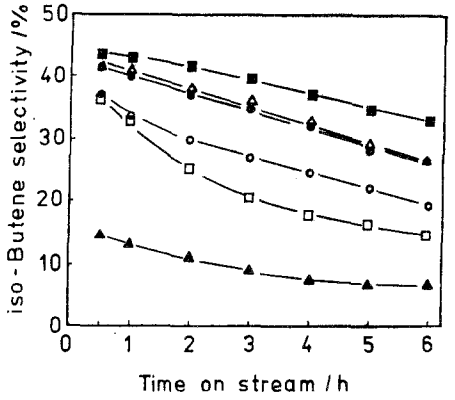

Fig. 5. Selectivity of isobutene formation versus time on stream at $T = 743$ K.(△) MnAPSO-31/2, (■) MnAPSO-31/1, (○) MnAPO-31/2, (□) MnAPSO-31/3, (●) SAPO-31, and (▲) $AlPO_4$-31, low template concentration. Reaction conditions: sample weight 1 g (35 wt% molecular sieve, 65 wt% SiO_2 binder), feed composition 50 vol% 1-butene, carrier gas nitrogen, overall flow rate 1 $cm^3 s^{-1}$.

decided at present whether this improvement simply comes about through the higher overall concentration of acid sites or through a cooperative effect between the two types of centres. Evidently, higher Mn contents lead to lower isobutene selectivities. Qualitatively, the loss of isobutene selectivity corresponds to the loss of activity (decrease of 1-butene conversion). Obviously, acid sites of higher strength are poisoned by coke during time on stream. From an industrial point of view, the formation of the double bond isomers does not represent a loss of 1-butene since the mixture of all three *n*-butenes can be recycled and each isomer can actually serve as reactant. For this purpose and for comparison with published patents the isobutene selectivity can alternatively be defined in the form:

$$\text{selectivity of isobutene (\%)} = 100\,(\text{isobutene})_{\text{out}}/[(\text{1-butene})_{\text{in}} - (\Sigma\{n\text{-butenes}\})_{\text{out}}].$$

These selectivity values range between 89.5% ($AlPO_4$-31) and 94.7% (MnAPSO-31/1) after 6 h. This underlines that even on the parent $AlPO_4$-31 structure the percentage of side reactions is rather low. Nevertheless, liquid products could be accumulated over 6 h in case of SAPO-31. This product contained mainly linear and branched higher alkenes and traces of substituted benzenes. The space-time-yield (STY) of isobutene for the best catalyst, MnAPSO-31/1, calculated with a WHSV of 4.5 g of 1-butene per gram of catalyst per hour yields a value of 3.2 g isobutene per gram of molecular sieve per hour after 6 h time on stream. For comparison, a catalyst consisting of γ-Al_2O_3 modified with 5.6% SiO_2 is reported to allow a STY of 0.25 at 765 K [9]. However, it has to be taken into account that the molecular sieve catalysts have not yet reached their steady state activity after 6 h and that a further decrease of the STY of isobutene can be expected. Nevertheless, it is obvious that Mn considerably suppresses deactivation tendencies of the catalyst samples.

4. Conclusions

(i) The formation of isobutene from 1-butene over substituted $AlPO_4$-31 molecular sieve catalysts proceeds with good selectivity. The catalyst performance is improved by a simultaneous incorporation of Mn and Si into the $AlPO_4$-31 structure.

(ii) The catalysts deactivate with time on stream where the modification with Mn considerably improves the resistance against coking.

(iii) The best results have been achieved with molecular sieve MnAPSO-31 and a MnO/P_2O_5 ratio of 0.01. The effect of varying the Si content has not yet been investigated.

(iv) The space-time-yield of isobutene calculated after 6 h time on stream is higher than reported for other catalyst systems under comparable conditions.

Acknowledgement

We are indebted to Mr. J. Richter-Mendau for taking the SEM photographs. MR thanks the "Fonds der Chemischen Industrie" for financial support.

References

[1] B.M. Lok, C.A. Messina, R.L. Patton, R.T. Gajek, T.R. Cannan and E.M. Flanigen, J. Am. Chem. Soc. 106 (1984) 6092.
[2] E.M. Flanigen, B.M. Lok, R.L. Patton and S.T. Wilson, in: *New Developments in Zeolite Science and Technology*, Proc. 7th Int. Zeolite Conf., eds. Y. Murakami, A. Iijima and J.W. Ward (Kodansha, Tokyo, 1986) p. 103.
[3] D.F. Cox and M.E. Davis, in: *Novel Materials in Heterogeneous Catalysis*, ACS Symp. Ser, Vol. 437, ed. R.T. Baker (Am. Chem. Soc., Washington, 1990) p. 38.
[4] J.A. Martens, C. Janssens, P.-J. Grobet, H.K. Beyer and P.A. Jacobs, in: *Zeolites: Facts, Figures, Future*, Proc. 8th Int. Zeolite Conf., eds. P.A. Jacobs and R.A. van Santen (Elsevier, Amsterdam, 1989) p. 215.
[5] N.B. Milestone and N.H.J. Tapp, in: *Methane Conversion*, eds. D.M. Bibby, C.D. Chang, R.F. Howe and S. Yurchak (Elsevier, Amsterdam, 1988) p. 553.
[6] E.M. Flanigen, R.L. Patton and S.T. Wilson, in: *Innovation in Zeolite Materials Science*, eds. P.J. Grobet, W.J. Mortier, E.F. Vansant and G. Schulz-Ekloff (Elsevier, Amsterdam, 1988) p. 13.
[7] J.M. Bennett and R.M. Kirchner, Zeolites 12 (1992) 338.
[8] H.-L. Zubowa, E. Alsdorf, R. Fricke, F. Neissendorfer, J. Richter-Mendau, E. Schreier, D. Zeigan and B. Zibrowius, J. Chem. Soc. Faraday Trans. 86 (1990) 2307.
[9] B. Schleppinghoff, A. Sinhuber and H. Mentzen, DE 3227676 , EC Erdölchemie GmbH, Germany (1984).
[10] G. Franz and H.-J. Ratajczak, DE 3000650, Chemische Werke Hüls AG, Germany (1982).
[11] Ju.G. Eguazarov, M.F. Savcic and E.Ja. Ustilovskaja, *Heterogeneously Catalyzed Isomerization of Hydrocarbons* (Nauka i Technika, Minsk, 1989) pp. 31 ff. (in Russian).
[12] B.M. Lok, A. Messina, R.L. Patton, R.T. Gajek, T.R. Cannan and E.M. Flanigen, US Patent 4 440 871.
[13] D. Timm, G. Öhlmann, R. Fricke, U. Roost, H.-L. Zubowa, K. Becker and H. Striegler, Patent DE 4139552, Leuna-Werke AG, Germany (1992).
[14] J. Fries and H. Getrost, *Organische Reagenzien für die Spurenanalyse* (Merck, Darmstadt, 1977) pp. 233 ff.
[15] M. Richter, E. Schreier and H.-L. Zubowa, J. Catal., submitted.
[16] G. Brouet, X. Chen, Ch.W. Lee and L. Kevan, J. Am. Chem. Soc. 114 (1992) 3720.